https://doi.org/10.5194/egusphere-2025-2027
Preprint. Discussion started: 4 June 2025
© Author(s) 2025. CC BY 4.0 License.

Impacts of shipping emissions on ozone pollution in China

Zhenyu Luo[#], Li Peng[#], Zhaofeng Lv, Tingkun He, Wen Yi, Yongyue Wang, Kebin He, Huan Liu*

State Key Laboratory of Regional Environment and Sustainability, School of Environment, Tsinghua University, Beijing 100084, China

[#] These authors contributed equally to this work.

* Correspondence: Huan Liu (liu_env@tsinghua.edu.cn)

Abstract

With the Two Phases of Clean Air Actions in China, the shipping sector has emerged as a significant source with substantial emission reduction potential compared to land-based anthropogenic sectors. Therefore, understanding the contribution of shipping emissions to ozone (O_3) pollution is therefore essential for advancing China's air pollution control efforts. In this study, a coupled framework including a chemical transport model with machine learning techniques was developed to systematically investigate the interannual and seasonal impacts of shipping emissions on O_3 concentrations across China during the period from 2016 to 2020, and explore mechanisms of shipping emissions influence O_3 formation. Results indicate that shipping emissions increases O_3 concentrations by a five-year average of 3.5 ppb nationwide, exhibiting significant spatial and temporal heterogeneity across different regions and seasons. Although significant differences exist between the emissions of ocean vessels and inland vessels, their contributions to O_3 formation are becoming increasingly comparable. Solely controlling shipping emissions may not necessarily result in effective O_3 mitigation. Instead, coordinated reductions targeting both shipping and land-based anthropogenic sources, along with region-specific and targeted emission control strategies, are critical for achieving substantial improvements in O_3 pollution mitigation.

https://doi.org/10.5194/egusphere-2025-2027
Preprint. Discussion started: 4 June 2025
© Author(s) 2025. CC BY 4.0 License.

1 Introduction

Over the past decades, China's rapid industrialization and urbanization have boost the economy but also exacerbated air pollution (Zhang et al., 2019). To address air pollution and the health burden from anthropogenic emissions, China introduced the Air Pollution Prevention and Control Action Plan in 2013 (Zheng et al., 2018). Although a serious of stringent measures have greatly improved $PM_{2.5}$ pollution in China, ozone (O_3) pollution has become increasingly prominent (Liu et al., 2023). Numerous epidemiological studies have shown that ground-level O_3 pollution leads to a range of adverse health effects, including increased incidence and mortality of respiratory diseases (Ito et al., 2005; Jerrett et al., 2009; Tao et al., 2012). Therefore, the health benefits achieved by reducing $PM_{2.5}$ pollution are partially offset by the increase in O_3 pollution (Xie et al., 2019; Wang et al., 2021), indicating a need to explore strategies to mitigate O_3 pollution in China.

With the promotion of China's emission control actions, the potential for further reductions from land anthropogenic emissions has diminished, while the shipping sector has shown considerable potential. Ships emit both gaseous and particulate pollutants, including sulfur dioxide (SO_2), nitrogen oxides (NO_x), particulate matter, and volatile organic compound (VOC). As the largest maritime trading nation, China has a higher share of shipping emissions among anthropogenic sources compared to international levels (Fu et al., 2017; Yi et al., 2025). Currently, shipping emission controls in China focus on reducing SO_2 and PM emissions through the adoption of low-sulfur fuels (Wang et al., 2021). With increasing trade volumes, however, shipping NO_x and VOC emissions continue to rise, and the use of low-sulfur fuel may further increase VOC emissions (Wu et al., 2020). Therefore, clarifying the historical and current contribution of shipping emissions to the formation of O_3 is critical important for further pollution control in China.

Previous studies have quantified the impacts of shipping emissions on O_3 pollution in China, particularly in the Yangtze River Delta (YRD), Pearl River Delta (PRD), and Bohai Rim Area (BRA) (Wang et al., 2019; Fu et al., 2023; Zheng et al., 2024). However, these studies predominantly focused on coastal areas, while the potential inland impacts are not well studied. Research has indicated that the air quality effects of inland shipping should not be neglected (Huang et al., 2022; Luo et al., 2024). The formation of O_3 exhibits strong spatial heterogeneity and is influenced by multiple factors, such as meteorological conditions and the emission intensities from both shipping and land-based sources. Currently, there is a lack of comprehensive studies employing a unified methodology to assess the nationwide impact of shipping emissions on ozone. Furthermore, previous studies were limited to restricted timeframes, resulting in a deficiency in comprehensive assessments of multi-year scenarios that encompass coordinated variations in both land and shipping emissions.

O_3 is generated by photochemical reactions between NO_x and VOC under solar radiation, thus, the impacts of shipping emissions on O_3 concentrations are attributed by the nonlinear response of O_3 to changes in NO_x and VOC emissions (P. Wang et al., 2019; Wang et al., 2017). However, previous studies commonly used the zero-out method to assess ship's impacts by comparing scenario differences simulated by chemical transport models, which does not fully involve the nonlinear response of O_3 to its precursors and would result in considerable

https://doi.org/10.5194/egusphere-2025-2027
Preprint. Discussion started: 4 June 2025
© Author(s) 2025. CC BY 4.0 License.

uncertainty in the evaluations. Furthermore, although model-based assessments can generate large amounts of simulation data to investigate the impacts of shipping emissions, current analyses struggle to struggles the mechanism of how shipping emissions contribute to ozone formation rom these simulation big data (Luo et al., 2025).

In this study, we conducted source-oriented chemical transport model with a spatial resolution of 36 km×36 km, to investigate the annual and seasonal impacts of shipping emissions on O_3 concentrations in China, especially for key coastal and inland regions from 2016 to 2020. We also allocate culpabilities of shipping emissions from ocean-going vessels (OGVs), coastal vessels (CVs), and river vessels (RVs) on O_3 pollution to identify the influences of regionally differentiated shipping emission control policies. Furthermore, an explainable machine learning model was applied to explore how shipping emissions affect the formation of O_3 based on five-years simulated data. Our study provides a nationwide and long-term analysis of the impacts shipping emissions on China's O_3 pollution, and provide new insights for shipping control measures in the future.

2 Methods

2.1 Shipping emissions

The Shipping Emission Inventory Model (SEIM v2.0) is a disaggregate dynamic method (Luo et al., 2025) driven by driven (a) the high-frequency ship Automatic Identification System (AIS) data, including signal time, coordinate location, navigational speed, and operating status, and (b) the integrated Ship Technical Specifications Database (STSD) (updated to 2020), which describes ship static properties, including vessel type, maximum designed speed, DWT and engine power. First, the originally collected raw AIS data and ship profile data from multiple sources are combined to form a ship activity database and STSD. Second, a route restoration module is applied for cross-land trajectory with a long distance in the AIS data, in which the 10 min linear interpolation will be applied on the shorted paths instead. Third, the instantaneous emission along with the movement of the ship's trajectory will be calculated based on the ship's static technical parameters, dynamic load changes, and extra parameters and factors. Finally, shipping emission inventory datasets will be established and used for visualization and analyses from multiple perspectives. In the SEIM, shipping emissions for both air pollutants (e.g., SO_2, PM, NO_x, CO and HC) and greenhouse gases (e.g., CO_2, CH_4 and N_2O) from the main engines, auxiliary engines and boilers were calculated, detailed information of SEIM is described in our previous study (Wang et al., 2021). Here, we calculated annual shipping emissions from 2016 to 2020 within 200 Nm from the Chinese mainland's territorial sea baseline.

In this study, vessels were classified as ocean-going vessels (OGVs), coastal vessels (CVs) and river vessels (RVs) for emission estimation according the following rules: (a) OGVs were identified by both valid IMO numbers and the Maritime Mobile Service Identity (MMSI) numbers, since they are mostly engaged in international trade following the management of the IMO. (b) RVs were identified by frequency distribution method based on the navigation trajectories for each vessel. Vessels with more than 50 % of the AIS signals throughout the entire year occurring on inland rivers (14–43° N, 104–130° E) were considered as RVs. (c) Finally, vessels that are not identified as OGVs or RVs are regarded as CVs. **Figure 1** shows

https://doi.org/10.5194/egusphere-2025-2027
Preprint. Discussion started: 4 June 2025
© Author(s) 2025. CC BY 4.0 License.

the interannual variation of shipping NO_x and VOC emissions from 2016 to 2020. Overall, the increasing trade demands and total cargo throughput of Chinese ports led to elevated levels of ship activities and consequently a sustained rise in shipping NO_x and VOC emissions, especially for OGVs. Additionally, the shift to low-sulfur fuels, which are typically richer in short-chain hydrocarbons (Wu et al., 2020), has contributed to a rise in shipping VOC emissions.

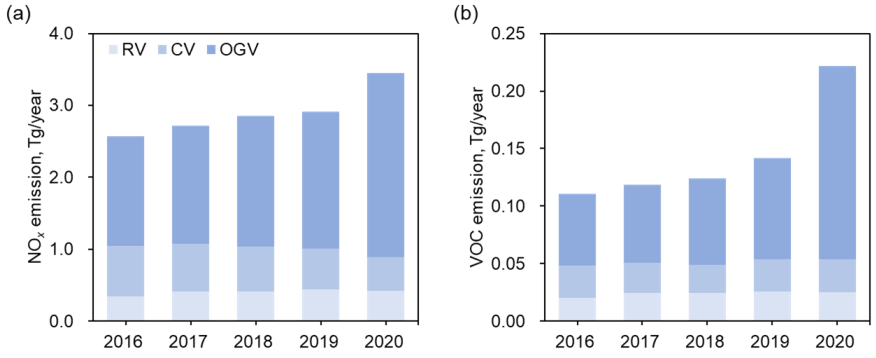

Figure 1. The interannual variation of shipping (a) NO_x and (b) VOC emissions from 2016 to 2020.

2.2 Air quality model

The Weather Research and Forecasting (WRF, version 3.8.1)−Community Multiscale Air Quality (CMAQ, version 5.4) model was applied to simulate the air quality in China during January, April, July and November from 2016 to 2020, which represented winter, spring, summer and fall, respectively, with 3 days of spin-up time for each run. As shown in **Figure S1**, the modeling domain covered all of China and some parts of East Asia with a horizontal resolution of 36 km × 36 km. Here, we have defined four key regions: BRA, YRD, PRD and inland river areas (IRA), in which we focus on shipping-related O_3 pollution.

Here the year of 2018 was regarded as a typical meteorological year since the climate for this year was relatively stable, and we used the meteorological filed of 2018 simulated by WRF in our previous study (Zhao et al., 2022) to drive the CMAQ simulation from 2016 to 2020. The first guess field and boundary conditions for WRF were generated from the 6 h NCEP FNL Operational Model Global Tropospheric Analyses dataset. The four-dimensional data assimilation (FDDA) was enabled using the NCEP ADP global surface and upper air observational weather data (http://rda.ucar.edu, last access: 25 March 2023). WRF and CMAQ used 32 vertical layers up to 100 hPa, and the lowest layer had a thickness of approximately 37 m. The major physical options in WRF included a Morrison two-moment microphysics scheme (Morrison et al., 2009), a Kain–Fritsch cumulus cloud parameterization (Kain, 2004), the Rapid Radiative Transfer Model (RRTM) longwave and shortwave radiation scheme (Iacono et al., n.d.), the Pleim–Xiu Land Surface Model (Xiu and Pleim, 2001), and the Asymmetric Convective Model version 3.0 for the PBL parameterization (Pleim, 2007). The validation of WRF performance is shown in **Table S1**.

Atmospheric gas-phase chemistry in the CMAQ was simulated with the SAPRC07tic

https://doi.org/10.5194/egusphere-2025-2027
Preprint. Discussion started: 4 June 2025
© Author(s) 2025. CC BY 4.0 License.

chemical mechanism, and aerosols were predicted using the AERO7. The chemical boundary conditions of CMAQ inputs were collected from the Community Atmosphere Model with Chemistry (CAM-chem) simulation output of global tropospheric and stratospheric compositions (Buchholz et al., 2019). In this study, the Integrated Source Apportionment Method (ISAM) was applied to determine the source contribution to the ambient O_3 concentrations. We divided the emissions into five groups to trace them separately in the ISAM, including the land-based anthropogenic emission (the mobiles, industry, power, domestic, and agriculture) from the MEIC and the open burning emissions Cai et al (Cai et al., 2017), the RVs' emission, the CVs' emission, the OGVs' emission, and the other emission (the nature sources emission from the MEGANv3 and the anthropogenic emission from other countries within the modeling domain from the MIX (Li et al., 2017), details of emissions are shown in **Table S2**.

We evaluated the simulated O_3 concentrations against ground-based observations for model validation. Until the simulation time, a total of 1455 available observation sites in China were used for O_3 validation. As shown in **Table S3**, the simulated O_3 agreed well with observations, with the overall model performance within the performance criteria suggested by Boylan and Russell (Boylan and Russell, 2006) (mean fractional bias (MFB) $\leq \pm 60$ % and mean fractional error (MFE) $\leq \pm 75$ %), while the model overestimated O_3 a little, mainly due to uncertainties in emission inventory and unavoidable deficiencies during meteorological and air quality simulation. Meteorological performance for simulated periods was described in our previous study (Zhao et al., 2022).

2.3 Explainable machine learning model

Here, based on the simulated data from 2016 to 2020 using WRF-CMAQ-ISAM, the RF model was used to simulated the monthly average O_3 concentration. In the RF model, the input predictor variables included relative humidity, temperature, wind speed, wind direction, solar radiation, land anthropogenic NO_x emissions, land anthropogenic VOC emissions, shipping NO_x emission and shipping VOC emission. Notably, the emissions selected were the sum of emissions from each grid and its eight neighboring grids.

To investigate the impact of shipping emissions on O_3 formation in different regions, we trained four RF models specifically for the BRA, YRD, PRD, and IRA regions, respectively. The simulation data from 2016 to 2019 were used as the training samples, while the simulation data from 2020, under the scenario of the most significant changes in shipping emissions, used as the test samples to validate the generalization capability of the RF models. By comparing the root mean squared error (RMSE) for testing datasets across models with candidate parameter combinations, we set mtry and NumTrees as 6 and 200 in RF, respectively. Additionally, the 10-fold cross-validation repeated 10 times was considered to evaluate the prediction performance of our models. The total dataset was randomly divided into 10 subsets, where 9 subsets was used to train the model and another was applied for validation. As shown in **Figure 2**. averages of RMSE and correlation coefficient (R2) in the CV of the RF models were 2.12~2.47 ppb, and 0.90~0.98, respectively, indicating an acceptable performance.

https://doi.org/10.5194/egusphere-2025-2027
Preprint. Discussion started: 4 June 2025
© Author(s) 2025. CC BY 4.0 License.

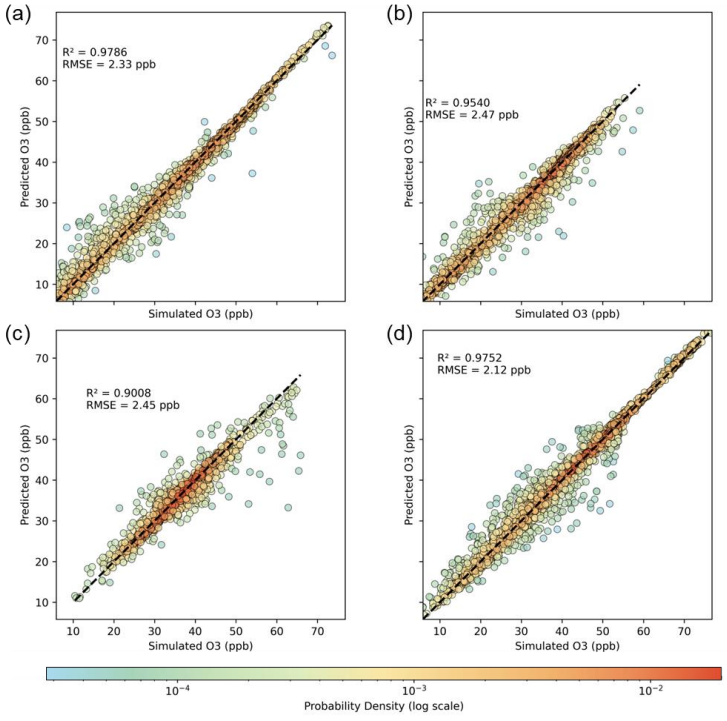

Figure 2. Performances of RF models for (a) BRA, (b) YRD, (c) PRD and (d) IRA.

In order to identify the sensitivity and response relationship between prediction variables and results in the RF models, the SHapley Additive exPlanations (SHAP) technique, a game-theoretic framework introduced by Lundberg et al. (Lundberg et al., 2020; Lundberg and Lee, 2017), was employed to interpret the RF models using the Python scikit-learn library. The SHAP approach enables the quantification of both global and local influences of input variables on the model's predictions, thereby improving the interpretability of factors contributing to air pollution. Additionally, the study examined feature interactions, which can affect the model's predictive accuracy, to gain a more comprehensive understanding of the intricate relationships among the variables.

3 Results and discussions

3.1 Annual O_3 impact from shipping emissions

Figure 3a shows the five-year average of shipping-related O_3, which is defined as the sum of O_3 concentration caused by emissions of OGVs, CVs, and RVs traced by CMAQ-ISAM. Overall, the shipping emissions increases O_3 concentrations by 3.5 ppb nationwide, showing a decrease trend from the southeast coast toward inland areas. This result is greater than the findings in other countries such as 1.97 ppb in Europe, and 2.08 ppb in the United States under ambient temperature and pressure (Sun et al., 2024). Due to the high coastal shipping emissions, the shipping-related O_3 could exceed 15 ppb in southeast coastal regions, especially in YRD and PRD, where maximum

https://doi.org/10.5194/egusphere-2025-2027
Preprint. Discussion started: 4 June 2025
© Author(s) 2025. CC BY 4.0 License.

values reach 25.4 ppb and 26.3 ppb, respectively. For the regions with low shipping emissions, the shipping-related O_3 is relatively low, not exceeding 5 ppb. For example, in IRA and BRA, the shipping-related O_3 is 3.9 ppb and 4.5 ppb respectively, but is slightly higher than the national average. Meteorological factors are just as important as anthropogenic emission influences in O_3 production (Liu et al., 2023; Zhang et al., 2024). The BRA and IRA have lower temperatures and weaker solar radiation compared to the YRD and PRD (Figure SX), which reduces the formation of hydroxyl radicals, weaking the atmospheric photochemical oxidizing capacity and ultimately limiting the O_3 production.

Figure 3b shows the five-year average of the relative contribution of shipping emissions to O_3. Nationwide, the shipping emissions accounts for a 9.9% increase in O_3, showing a similar decreasing trend of from the southeast coast to inland regions. This result is higher than 3.7% reported for the Mediterranean region in 2015 (Fink et al., 2023), but lower than the 12-21% reported in another European study for 2010 (Lupascu and Butler, 2019). Notably, some coastal cities exhibit particularly high values. For example, in PRD region, the relative shipping-related O_3 exceeds 30.4% in Shenzhen, Guangdong Province. The IRA is relatively low at 10.4%, mainly because of the higher background O_3 concentrations from land-based anthropogenic sources or O_3 already formed by chemical reactions at sea and subsequently transported inland by onshore winds (Cheng et al., 2023).

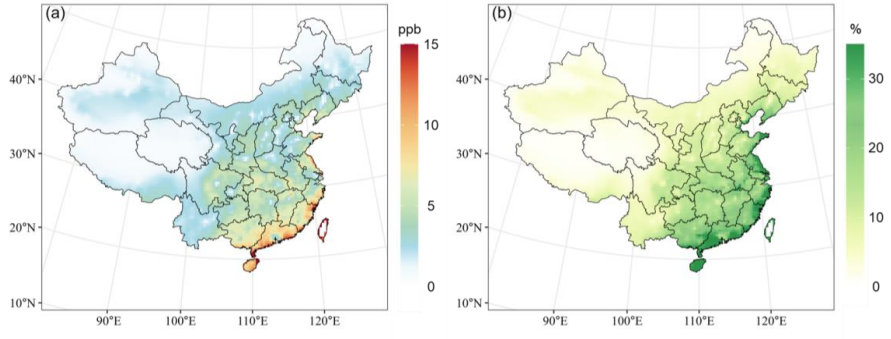

Figure 3. Contributions of shipping emissions to the five-year average O_3 pollution, including (a) absolute contributions and (b) relative contributions. Maps created with MeteoInfoMap (http://www.meteothink.org).

Figure 4 illustrates the interannual trend in shipping-related O_3 in key regions from 2016 to 2020. Overall, the shipping-related O_3 shows a slight upward trend, with an average annual growth rate of 0.54%, which is lower than the increases in shipping-related NO_x and VOC (**Figure 1**). This finding suggests that O_3 formation is not highly sensitive to ship emissions. Because O_3 is produced by photochemical reactions of NO_x and VOC in the presence of solar radiation, influenced by factors such as meteorological conditions, anthropogenic emissions, and long-range transport (Ye et al., 2023). Its response to shipping emissions is complex. The Chinese government's two phases of clean air actions (Phase I, 2013–2017; Phase II, 2018–2020) resulted in increasing trend of O_3 nationwide (Liu et al., 2023), and the relative contribution of shipping emissions to O_3 also rose

https://doi.org/10.5194/egusphere-2025-2027
Preprint. Discussion started: 4 June 2025
© Author(s) 2025. CC BY 4.0 License.

slightly during the same period.

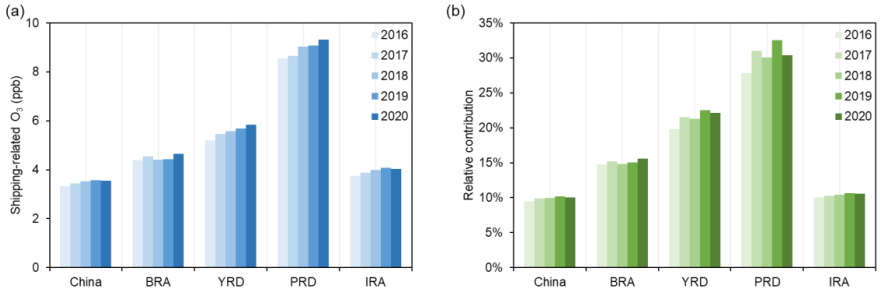

Figure 4. The interannual trend in shipping-related O_3, including (a) absolute contributions and (b) relative contributions, in key regions from 2016 to 2020.

3.2 Contribution of different types of vessels

We further investigated the relationship between O_3 pollution and shipping emissions from sub-ship sectors. **Figure 5** shows the spatial distribution of the five-year average contribution of emissions from different ship types to the shipping-related O_3. In coastal regions, OGVs contribute most to the shipping-related O_3, accounting for more than 50% of such O_3 pollution. CVs are the second-largest contributor to O_3 pollution with an average contribution of 20-30%, and contribute up to 40% in the southern coastal regions near Zhejiang and Fujian Provinces. Due to the regional transport and some RVs sail on coastal regions, contributions from RVs can also reach 20-30%. In inland regions, RVs remain the main source of shipping-related O_3, with contributions in the middle reaches of the Yangtze River reaching 50%.

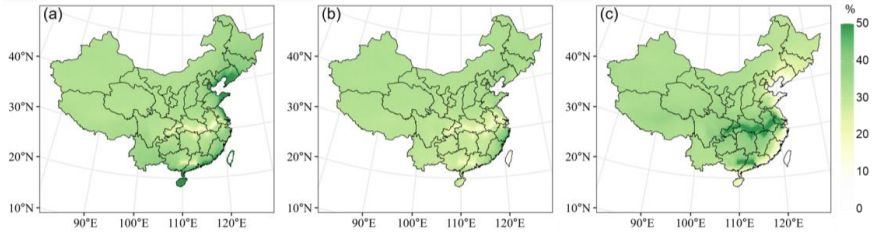

Figure 5. Contributions of emissions from (a) OGVs, (b) CVs, and (c) RVs to the five-year average shipping-related O_3 pollution. Maps created with MeteoInfoMap (http://www.meteothink.org).

The interannual variation in the contribution of the different types of ship to shipping-related O_3 between 2016 and 2020 for different regions is illustrated in **Figure 6**. Nationwide, the contribution of OGVs and RVs increased by 2.7% and 0.6%, respectively, while the contribution of CVs decreased by 3.3%. This pattern was observed in all coastal regions and IRA. The interannual variation in the contribution of the different types of ship to shipping-related O_3 follows a similar pattern to that of shipping-related NOx and VOC (**Figure 1**), particularly NOx emissions, which shows an upward trend for OGVs and RVs but a downward trend for CVs. As a result, the difference

https://doi.org/10.5194/egusphere-2025-2027
Preprint. Discussion started: 4 June 2025
© Author(s) 2025. CC BY 4.0 License.

in the contribution of different types of ships to air quality is gradually narrowing. Notably, although RVs emissions significantly less than those of OGVs and CVs, its contribution to O_3 is comparable to that of other ship types, even exceeds that of CVs in some coastal regions. In addition, although China has required certain categories of ships to install AIS equipment since 2010, a large part of small RVs in China have not been equipped with AIS (Zhang et al., 2017), which is not considered in this study. This result suggests the importance of paying greater attention to RVs in future emission control strategies.

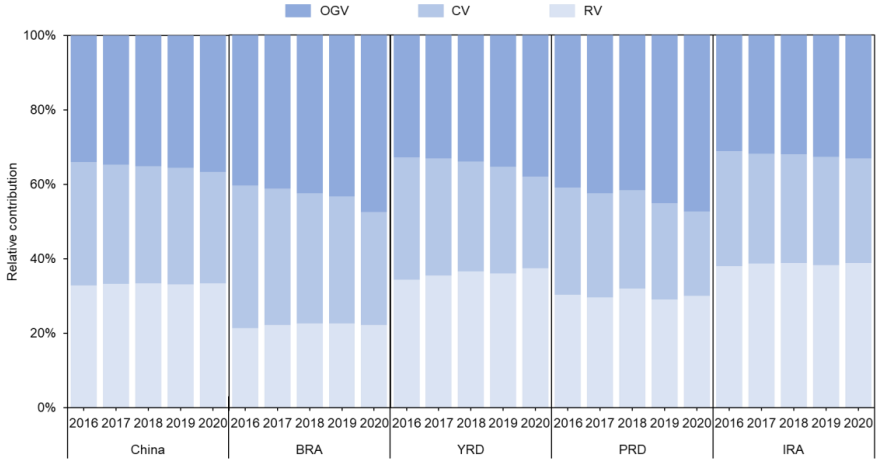

Figure 6. The interannual trend in Contributions of emissions from OGVs, CVs, and RVs to shipping-related O_3 in key regions from 2016 to 2020.

3.3 Seasonal O_3 impact from shipping emissions

The seasonal variation in the contribution of ship emissions to O_3 concentrations across the continent is shown in **Figure 7**, with January, April, July, and November representing winter, spring, summer, and fall, respectively. The relative contributions of ship emissions to O_3 in different seasons are presented in **Figure S3**. Overall, the contributions of ship emissions to O_3 concentrations in China were 1.53 ppb (5.6%), 4.24 ppb (9.8%), 4.77 ppb (13.7%), and 2.41 ppb (7.9%) for January, April, July, and November, respectively, which affected by the prevailing wind direction (**Figure S4**) and atmospheric oxidizing properties.

For cold seasons, including winter and fall, the shipping-related O_3 remains relatively low, primarily due to less irradiation and lower temperatures (**Figure S5**). Consequently, most regions remain under 5 ppb, except in the south of YRA, especially Guangdong and Hainan Provinces, where shipping-related O_3 exceeds 5 ppb (**Figure 7a and 7d**). During winter and fall, when the wind direction is mainly north and northeast, shipping-related pollutants are transported to the sea, limiting the accumulation of O_3 on land (Cheng et al., 2023). However, shipping-related O_3 in fall is slightly higher than in winter, mainly because the persistent and intense solar radiation after the rainy summer season enhances O_3 formation. Another reason for this is that during the winter months, mainland China is under the influence of the Mongolian High Pressure System, where continental winds reduce the shipping-related O_3

https://doi.org/10.5194/egusphere-2025-2027
Preprint. Discussion started: 4 June 2025
© Author(s) 2025. CC BY 4.0 License.

(Cheng et al., 2023; Zhao et al., 2023).

Warm seasons generally include spring and summer. In spring, shipping-related O_3 is highest in in coastal areas, particularly across Guangdong, Fujian, and Zhejiang Provinces, where it exceeds 15 ppb (**Figure 7b**). During this season, increasing solar radiation and moderate temperatures can enhance photochemical reactions, thereby promoting O_3 formation in these coastal areas. In summer, shipping emissions significantly increased O_3 concentrations nationwide (**Figure 7c**). Most coastal regions near the BRA and the PRD recorded levels above 10 ppb, while central China, located hundreds of kilometers from the coast, was still significantly impacted with average level of around 10 ppb. This is primarily because central China lies in a perennial monsoon region, where summer monsoons can carry shipping-related air pollutants inland from coastal cities (Zheng et al., 2024). Notably, the impact of ship emissions on O_3 in PRD reaches its highest contribution in spring rather than summer, consistent with the results of previous studies (Cheng et al., 2023; Schwarzkopf et al., 2022). The possible reason for this is that in PRD, particularly Fujian and Guangdong Provinces, experiences high humidity and frequent precipitation in summer (**Figure S6**), which decreases both O_3 concentrations and the impact of shipping emissions, even though high temperatures can promote photochemical activity. Strong onshore winds also play a role in reducing the influence of shipping emissions (Cheng et al., 2023; Ma et al., 2022).

These findings indicate that seasonal variations for shipping-related O_3 are driven by meteorological factors, particularly changes in prevailing wind direction, which are crucial for the diffusion and long-range transport of shipping emissions. Researchers suggest that the mixing emissions between shipping and local anthropogenic emissions can amplify complicated O_3 chemical formation in coastal cities (R. Wang et al., 2019). Therefore, seasonal mitigation strategies and a better understanding of regional monsoon dynamics and their interaction with local anthropogenic emissions are crucial for effectively reducing shipping-related O_3 pollution.

https://doi.org/10.5194/egusphere-2025-2027
Preprint. Discussion started: 4 June 2025
© Author(s) 2025. CC BY 4.0 License.

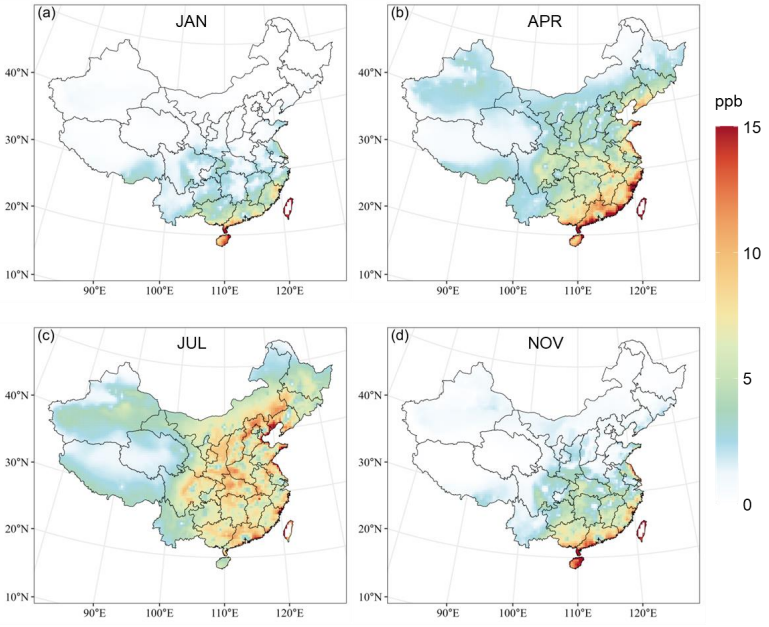

Figure 7. Contributions of shipping emissions to the seasonal mean O_3 concentrations for (a) winter (JAN), (b) spring (APR), (c) summer (JUL), and (d) fall (NOV). Maps created with MeteoInfoMap (http://www.meteothink.org).

3.4 Effects of shipping emission on O_3 formation

Although the features in the RF model include both meteorological factors and emissions, this section focuses on impacts of anthropogenic emissions, especially shipping emissions, on O_3 pollution. **Figure 8** presents the SHAP summary plots for selected features in the RF model for BRA, YRD, PRD, and IRA, showing the magnitude, prevalence, and direction of each feature's impact on the model output (O_3 concentration). In the summary plot, the further a feature's SHAP value is from zero, the greater its influence; positive SHAP values indicate a positive contribution, while negative values indicate a negative effect. For example, in **Figure 8a**, land-based NO_x and VOC emissions both have a significant impact on O_3 formation in the BRA, with contributions of 16.8% and 11.0%, respectively, suggesting that the atmospheric chemistry in this area is significantly affected by land-based anthropogenic emissions. Moreover, lower NO_x and VOC emissions leads to higher SHAP values, indicating a negative correlation between land-based anthropogenic emissions and O_3 pollution. In the coastal areas of BRA, shipping emissions are much smaller than land-based emissions, therefore, contribute only approximately 2.9% to O_3 formation, and exhibit a similar negative correlation as land-based sources.

As the share of shipping emissions increases within total anthropogenic emissions in the coastal areas of YRD and PRD, the difference between the contributions of shipping and land-

https://doi.org/10.5194/egusphere-2025-2027
Preprint. Discussion started: 4 June 2025
© Author(s) 2025. CC BY 4.0 License.

based emissions to O_3 pollution regions decreases. Especially in the PRD, shipping NO_x contributes up to 9.7%, exceeding the land-based VOC contribution of 5.3%. In the IRA, emissions from inland vessels are much lower than those from ocean-going and coastal ships, thus, shipping NO and VOC contributions only 1.5% and 0.8% to O_3 pollution, respectively.

For meteorological factors, the contributions of solar radiation (25.2%), temperature (20.0%), wind speed (11.5%), and wind direction (4.9%), relative humidity (4.8%) to O_3 formation exhibit clear regional heterogeneity. Overall, meteorological influences are greater than those of shipping emissions. This may be attributed to the highly complex physical and chemical processes involved, including cloud–radiation interactions, air mass transport, and water-related reactions.

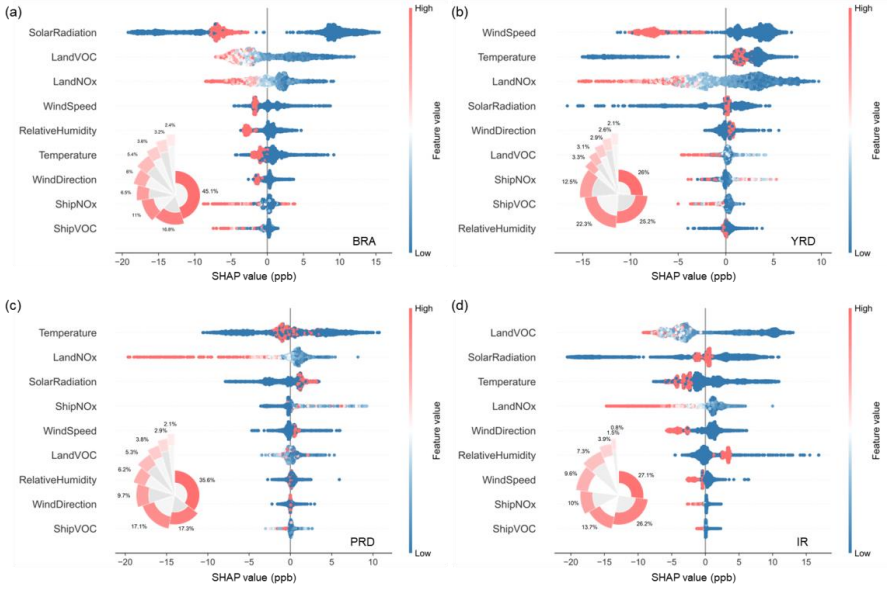

Figure 8. Feature importance results of the random forest regression model for (a) BRA, (b) YRD, (c) PRD, and (d) IRA.

The dependence plot (**Figure. 9**) further quantifies how changes in shipping emissions affect O_3 concentrations. Notably, due to the uneven distribution of shipping emissions, the x-axis in **Figure. 9** is set to non-uniform intervals to better illustrate their impact. Overall, as previously mentioned, changes in shipping NO_x and VOC emissions have a relatively minor effect on regional O_3 levels—approximately between –2.5 ppb to 8 ppb—although there is clear regional heterogeneity. In the BRA region, shipping emissions are negatively correlated with O_3, with increases in shipping NO_x and VOC emissions leading to a reduction of about 1–2 ppb in O_3. Differently, in the YRD and PRD, increases in shipping NO_x emissions slightly promote O_3 formation-especially in the PRD region, where O_3 may increase by up to 3 ppb, which is opposite to the impact of land-based NO_x emissions (**Figure. S7**). This difference may be

https://doi.org/10.5194/egusphere-2025-2027
Preprint. Discussion started: 4 June 2025
© Author(s) 2025. CC BY 4.0 License.

because, in the YRD and PRD, land-based NO_x emissions do not dominate the overall anthropogenic emissions as they do in the BRA, allowing shipping NO_x to also influence atmospheric chemistry. Furthermore, changes in shipping VOC emissions have almost no impact, consistent with the effect of changes in land-based VOC emissions (**Figure. S7**). Only when shipping VOC emissions increase dramatically in the YRD region is O_3 formation suppressed—though such cases are rare, as reflected by the partially negative SHAP values for shipping VOC emissions in **Figure. 8b**. In the IRA, similar to the BRA region, shipping emissions are very small compared to land-based sources, so that changes in shipping NO_x and VOC emissions have a similar negative effect on O_3 as those from land-based sources.

It should be noted that if one seeks to determine whether a given variable promotes or suppresses O_3 pollution using machine learning methods, additional field observations, experimental data, and corresponding simulation results may be required as supporting evidence. Considering the interactions among variables, even if individual contributions are small, the SHAP estimates for each explanatory variable are unlikely to perfectly reflect their actual contributions in the underlying physical processes.

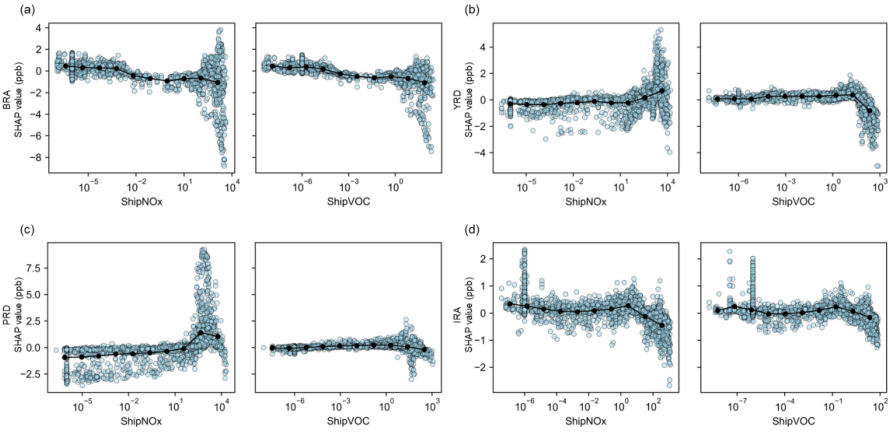

Figure 9. SHAP dependence plot for (a) BRA, (b) YRD, (c) PRD, and (d) IRA.

4 Conclusion

Overall, the shipping emissions increases O_3 concentrations by 3.5 ppb nationwide, with a significant spatial and temporal heterogeneity. The air quality in Chinese coastal cities is highly impacted by shipping emissions. For example, the relative shipping-related O_3 exceeds 26.3 ppb (30.4%) in PRD, while is relatively low at 3.9 ppb (10.4%) in IRA. Such pollution is more serious in warm seasons with an average of 4.77 ppb (13.7%) nationwide in summer, due to the increased solar radiation and moderate temperatures. although OGVs, CVs, and RVs exhibit significant differences in their emissions, the difference in their contributions to O_3 pollution are diminishing and becoming relatively comparable on a national scale.

To mitigate O_3 pollution, it is important to coordinate the control of shipping emissions

https://doi.org/10.5194/egusphere-2025-2027
Preprint. Discussion started: 4 June 2025
© Author(s) 2025. CC BY 4.0 License.

with land-based emission sources. The results show that the impact of shipping NO_x and VOC emissions on O_3 formation exhibits significant regional differences. In areas where land-based emissions dominate, such as the BRA region, the impact of shipping emissions on O_3 pollution is relatively small and shows a negative correlation. In contrast, in coastal regions such as the YRD and PRD, where the share of land-based emissions has decreased, the contribution of shipping emissions to O_3 formation becomes more significant. In particular, s shipping NO_x emissions have become an important source of O_3 precursors in the PRD region. This regional difference suggests that solely controlling shipping emissions may lead to unexpected atmospheric chemical responses and, under certain conditions, could even cause an increase in O_3 concentrations. Therefore, effective O_3 pollution control requires a coordinated reduction of both land-based and shipping emissions, based on regional emission structures and atmospheric oxidation characteristics. Further analysis reveals that meteorological conditions play an even more critical role in regulating O_3 formation. Variables such as solar radiation, temperature, wind speed, and relative humidity show strong sensitivity to changes in O_3 concentration and also display clear regional differences. Therefore, it is recommended that differentiated and refined joint control strategies be developed for different regions based on their specific emission characteristics and meteorological conditions.

Data availability

Data used during the current study are available from the corresponding author upon reasonable request.

Code availability

Codes used during the current study are available from the corresponding author upon reasonable request.

Acknowledgments

This research has been supported by: National Natural Science Foundation of China (grant nos. 42325505 to H.L.), National Key Research and Development Program of China (grant no. 2022YFC3704200 to H.L.), National Natural Science Foundation of China (grant no. 42405097 to Z.Lv).

Author Contributions

Conceptualization: Z.Luo, L.P., H.L.; Methodology: Z.Luo, Z.Lv; Investigation: W.Y., T.H., Y.W; Visualization: Z.L.uo L.P.; Supervision: H.L., K.H.; Writing—original draft: Z.Luo, L.P.; Writing—review & editing: Z.Luo, H.L.

https://doi.org/10.5194/egusphere-2025-2027
Preprint. Discussion started: 4 June 2025
© Author(s) 2025. CC BY 4.0 License.

Declaration of interests

The authors declare no competing interests.

Reference

Boylan, J.W., Russell, A.G., 2006. PM and light extinction model performance metrics, goals, and criteria for three-dimensional air quality models. Atmos. Environ., Special issue on Model Evaluation: Evaluation of Urban and Regional Eulerian Air Quality Models 40, 4946–4959. https://doi.org/10.1016/j.atmosenv.2005.09.087

Buchholz, R.R., Emmons, L.K., Tilmes, S., The CESM2 Development Team, 2019. CESM2.1/CAM-chem instantaneous output for boundary conditions. https://doi.org/10.5065/NMP7-EP60

Cai, S., Wang, Y., Zhao, B., Wang, S., Chang, X., Hao, J., 2017. The impact of the "air pollution prevention and control action plan" on PM2.5 concentrations in jing-jin-ji region during 2012–2020. Sci. Total Environ. 580, 197–209. https://doi.org/10.1016/j.scitotenv.2016.11.188

Cheng, Q., Wang, X., Chen, D., Ma, Y., Zhao, Y., Hao, J., Guo, X., Lang, J., Zhou, Y., 2023. Impact of ship emissions on air quality in the guangdong-hong kong-macao greater bay area (GBA): With a particular focus on the role of onshore wind. Sustainability 15, 8820. https://doi.org/10.3390/su15118820

Fink, L., Karl, M., Matthias, V., Oppo, S., Kranenburg, R., Kuenen, J., Moldanova, J., Jutterstrom, S., Jalkanen, J.-P., Majamaki, E., 2023. Potential impact of shipping on air pollution in the Mediterranean region - a multimodel evaluation: comparison of photooxidants NO_2 and O_3. Atmos. Chem. Phys. 23, 1825–1862. https://doi.org/10.5194/acp-23-1825-2023

Fu, M., Liu, H., Jin, X., He, K., 2017. National- to port-level inventories of shipping emissions in China. Environ. Res. Lett. 12, undefined-undefined. https://doi.org/10.1088/1748-9326/aa897a

Fu, X., Chen, D., Wang, X., Li, Y., Lang, J., Zhou, Y., Guo, X., 2023. The impacts of ship emissions on ozone in eastern China. Science of the Total Environment 903, 166252.

Huang, H., Zhou, C., Huang, L., Xiao, C., Wen, Y., Li, J., Lu, Z., 2022. Inland ship emission inventory and its impact on air quality over the middle yangtze river, china. Sci. Total Environ. 843, 156770. https://doi.org/10.1016/j.scitotenv.2022.156770

Iacono, M.J., Delamere, J.S., Mlawer, E.J., Shephard, M.W., Clough, S.A., Collins, W.D., n.d. Radiative forcing by long-lived greenhouse gases: calculations with the AER radiative transfer models. https://doi.org/10.1029/2008JD009944

Ito, K., De Leon, S.F., Lippmann, M., 2005. Associations between ozone and daily mortality: analysis and meta-analysis. Epidemiology 16, 446-457

Jerrett, M., Burnett, R.T., Pope III, C.A., Ito, K., Thurston, G., Krewski, D., Shi, Y., Calle, E., Thun, M., 2009. Long-term ozone exposure and mortality. New England Journal of Medicine 360, 1085-1095

Kain, J.S., 2004. The kain–fritsch convective parameterization: an update.

Li, M., Zhang, Q., Kurokawa, J., Woo, J.-H., He, K., Lu, Z., Ohara, T., Song, Y., Streets, D.G.,

https://doi.org/10.5194/egusphere-2025-2027
Preprint. Discussion started: 4 June 2025
© Author(s) 2025. CC BY 4.0 License.

Carmichael, G.R., Cheng, Y., Hong, C., Huo, H., Jiang, X., Kang, S., Liu, F., Su, H., Zheng, B., 2017. MIX: a mosaic asian anthropogenic emission inventory under the international collaboration framework of the MICS-asia and HTAP. Atmos. Chem. Phys. 17, 935–963. https://doi.org/10.5194/acp-17-935-2017

Liu, Yuxi, Geng, G., Cheng, J., Liu, Yang, Xiao, Q., Liu, L., Shi, Q., Tong, D., He, K., Zhang, Q., 2023. Drivers of increasing ozone during the two phases of clean air actions in China 2013–2020. Environ. Sci. Technol. 57, 8954–8964. https://doi.org/10.1021/acs.est.3c00054

Lundberg, S.M., Erion, G., Chen, H., DeGrave, A., Prutkin, J.M., Nair, B., Katz, R., Himmelfarb, J., Bansal, N., Lee, S.-I., 2020. From local explanations to global understanding with explainable AI for trees. Nat. Mach. Intell. 2, 56–67. https://doi.org/10.1038/s42256-019-0138-9

Lundberg, S.M., Lee, S.-I., 2017. A unified approach to interpreting model predictions, in: Proceedings of the 31st International Conference on Neural Information Processing Systems, NIPS'17. Curran Associates Inc., Red Hook, NY, USA, pp. 4768–4777.

Luo, Z., He, T., Lv, Z., Zhao, J., Zhang, Z., Wang, Y., Yi, W., Lu, S., He, K., Liu, H., 2025. Insights into transportation CO2 emissions with big data and artificial intelligence. Patterns 101186. https://doi.org/10.1016/j.patter.2025.101186

Luo, Z., Lv, Z., Zhao, J., Sun, H., He, T., Yi, W., Zhang, Z., He, K., Liu, H., 2024. Shipping-related pollution decreased but mortality increased in Chinese port cities. Nat Cities 1, 295–304. https://doi.org/10.1038/s44284-024-00050-8

Lupascu, A., Butler, T., 2019. Source attribution of european surface O_3 using a tagged O_3 mechanism. Atmos. Chem. Phys. 19, 14535–14558. https://doi.org/10.5194/acp-19-14535-2019

Ma, Y., Chen, D., Fu, X., Shang, F., Guo, X., Lang, J., Zhou, Y., 2022. Impact of sea breeze on the transport of ship emissions: A comprehensive study in the bohai rim region, China. Atmosphere 13, 1094. https://doi.org/10.3390/atmos13071094

Morrison, H., Thompson, G., Tatarskii, V., 2009. Impact of cloud microphysics on the development of trailing stratiform precipitation in a simulated squall line: comparison of one- and two-moment schemes. https://doi.org/10.1175/2008MWR2556.1

Pleim, J.E., 2007. A combined local and nonlocal closure model for the atmospheric boundary layer. Part I: model description and testing. https://doi.org/10.1175/JAM2539.1

Schwarzkopf, D.A., Petrik, R., Matthias, V., Quante, M., Yu, G., Zhang, Y., 2022. Comparison of the impact of ship emissions in northern europe and eastern China. Atmosphere 13, 894. https://doi.org/10.3390/atmos13060894

Sun, W., Jiang, W., Li, R., 2024. Global health benefits of shipping emission reduction in early 2020. Atmos. Environ. 333, 120648. https://doi.org/10.1016/j.atmosenv.2024.120648

Tao, Y., Huang, W., Huang, X., Zhong, L., Lu, S.-E., Li, Y., Dai, L., Zhang, Y., Zhu, T., 2012. Estimated acute effects of ambient ozone and nitrogen dioxide on mortality in the Pearl River Delta of southern China. Environmental health perspectives 120, 393-398.

Wang, F., Qiu, X., Cao, J., Peng, L., Zhang, N., Yan, Y., Li, R., 2021. Policy-driven changes in

https://doi.org/10.5194/egusphere-2025-2027
Preprint. Discussion started: 4 June 2025
© Author(s) 2025. CC BY 4.0 License.

the health risk of PM2. 5 and O3 exposure in China during 2013–2018. Science of The Total Environment 757, 143775.

Wang, P., Chen, Y., Hu, J., Zhang, H., Ying, Q., 2019. Attribution of tropospheric ozone to NOx and VOC emissions: considering ozone formation in the transition regime. Environ. Sci. Technol. 53, 1404–1412. https://doi.org/10.1021/acs.est.8b05981

Wang, R., Tie, X., Li, G., Zhao, S., Long, X., Johansson, L., An, Z., 2019. Effect of ship emissions on O_3 in the Yangtze River delta region of China: analysis of WRF-chem modeling. Sci. Total Environ. 683, 360–370. https://doi.org/10.1016/j.scitotenv.2019.04.240

Wang, T., Xue, L., Brimblecombe, P., Lam, Y.F., Li, L., Zhang, L., 2017. Ozone pollution in China: a review of concentrations, meteorological influences, chemical precursors, and effects. Sci. Total Environ. 575, 1582–1596. https://doi.org/10.1016/j.scitotenv.2016.10.081

Wang, X., Yi, W., Lv, Z., Deng, F., Zheng, S., Xu, H., Zhao, J., Liu, H., He, K., 2021. Ship emissions around china under gradually promoted control policies from 2016 to 2019. Atmos. Chem. Phys. 21, 13835–13853. https://doi.org/10.5194/acp-21-13835-2021

Wu, Z., Zhang, Y., He, J., Chen, H., Huang, X., Wang, Y., Yu, X., Yang, W., Zhang, R., Zhu, M., Li, S., Fang, H., Zhang, Z., Wang, X., 2020. Dramatic increase in reactive volatile organic compound (VOC) emissions from ships at berth after implementing the fuel switch policy in the pearl river delta emission control area. Atmos. Chem. Phys. 20, 1887–1900. https://doi.org/10.5194/acp-20-1887-2020

Xie, Y., Dai, H., Zhang, Y., Wu, Y., Hanaoka, T., Masui, T., 2019. Comparison of health and economic impacts of PM2. 5 and ozone pollution in China. Environment international 130, 104881

Xiu, A., Pleim, J.E., 2001. Development of a land surface model. Part I: application in a mesoscale meteorological model.

Ye, C., Lu, K., Ma, X., Qiu, W., Li, S., Yang, X., Xue, C., Zhai, T., Liu, Y., Li, X., Li, Y., Wang, H., Tan, Z., Chen, X., Dong, H., Zeng, L., Hu, M., Zhang, Y., 2023. HONO chemistry at a suburban site during the EXPLORE-YRD campaign in 2018: formation mechanisms and impacts on O_3 production. Atmos. Chem. Phys. 23, 15455–15472. https://doi.org/10.5194/acp-23-15455-2023

Yi, W., Wang, X., He, T., Liu, H., Luo, Z., Lv, Z., He, K., 2025. The high-resolution global shipping emission inventory by the shipping emission inventory model (SEIM). Earth Syst. Sci. Data 17, 277–292. https://doi.org/10.5194/essd-17-277-2025

Zhang, L., Wang, L., Ji, D., Xia, Z., Nan, P., Zhang, J., Li, K., Qi, B., Du, R., Sun, Y., Wang, Y., Hu, B., 2024. Explainable ensemble machine learning revealing the effect of meteorology and sources on ozone formation in megacity hangzhou, china. Sci. Total Environ. 922, 171295. https://doi.org/10.1016/j.scitotenv.2024.171295

Zhang, Q., Zheng, Y., Tong, D., Shao, M., Wang, S., Zhang, Y., Xu, X., Wang, J., He, H., Liu, W., Ding, Y., Lei, Y., Li, J., Wang, Z., Zhang, X., Wang, Y., Cheng, J., Liu, Y., Shi, Q., Yan, L., Geng, G., Hong, C., Li, M., Liu, F., Zheng, B., Cao, J., Ding, A., Gao, J., Fu, Q., Huo, J., Liu, B., Liu, Z., Yang, F., He, K., Hao, J., 2019. Drivers of improved PM2.5 air quality in China from 2013 to 2017. Proc. Natl. Acad. Sci. U. S. A. 116,

https://doi.org/10.5194/egusphere-2025-2027
Preprint. Discussion started: 4 June 2025
© Author(s) 2025. CC BY 4.0 License.

24463–24469. https://doi.org/10.1073/pnas.1907956116

Zhang, Y., Yang, X., Brown, R., Yang, L., Morawska, L., Ristovski, Z., Fu, Q., Huang, C., 2017. Shipping emissions and their impacts on air quality in China. Sci. Total Environ. 581–582, 186–198. https://doi.org/10.1016/j.scitotenv.2016.12.098

Zhao, C.-B., Li, Q.-Q., Nie, Y., Wang, F., Xie, B., Dong, L.-L., Wu, J., 2023. The reversal of surface air temperature anomalies in China between early and late winter 2021/2022: Observations and predictions. Advances in Climate Change Research 14, 660–670. https://doi.org/10.1016/j.accre.2023.09.004

Zhao, J., Lv, Z., Qi, L., Zhao, B., Deng, F., Chang, X., Wang, X., Luo, Z., Zhang, Z., Xu, H., Ying, Q., Wang, S., He, K., Liu, H., 2022. Comprehensive assessment for the impacts of S/IVOC emissions from mobile sources on SOA formation in China. Environ. Sci. Technol. 56, 16695–16706. https://doi.org/10.1021/acs.est.2c07265

Zheng, B., Tong, D., Li, M., Liu, F., Hong, C., Geng, G., Li, H., Li, X., Peng, L., Qi, J., Yan, L., Zhang, Y., Zhao, H., Zheng, Y., He, K., Zhang, Q., 2018. Trends in China's anthropogenic emissions since 2010 as the consequence of clean air actions. Atmos. Chem. Phys. 18, 14095–14111. https://doi.org/10.5194/acp-18-14095-2018

Zheng, S., Jiang, F., Feng, S., Liu, H., Wang, X., Tian, X., Ying, C., Jia, M., Shen, Y., Lyu, X., Guo, H., Cai, Z., 2024. Impact of marine shipping emissions on ozone pollution during the warm seasons in China. J. Geophys. Res.: Atmos. 129, e2024JD040864. https://doi.org/10.1029/2024JD040864